EKSPLOATACJA I NIEZAWODNOŚĆ MAINTENANCE AND RELIABILITY

Eksploatacja i Niezawodnosc – Maintenance and Reliability

Volume 22 (2020), Issue 4

journal homepage: http://www.ein.org.pl

Article citation info:
Li J-H, Liu Z-J, Wang D-P, Tian Y, Zhao Y-C. Fault mode analysis and reliability optimization design of a mechanical interface based on cylindrical cam mechanisms. Eksploatacja i Niezawodnosc – Maintenance and Reliability 2020; 22 (4): 715–723, http://dx.doi.org/10.17531/ein.2020.4.15.

Indexed by: Web of Science Group

Fault mode analysis and reliability optimization design of a mechanical interface based on cylindrical cam mechanisms

Jian-Hao Li [a], Zhi-Jie Liu [a]*, Da-Peng Wang [b], Yun Tian [b], Yu-Chong Zhao [a]

[a] Naval Architecture and Ocean Engineering College, Dalian Maritime University, Dalian, Liaoning, 116026, P.R. China
[b] Beijing Spacecrafts, Beijing, 100083, P.R. China

Highlights

- The motion fault modes of a mechanical interface based on coupled cylindrical cam mechanisms were presented.
- The performance functions of the interface are established for analyzing the motion faults based on Monte Carlo simulation.
- The fault probability of the interface is inversely proportional to the rotation speed of the drive ring. When the protrusion length of the interface case is extended to 3-3.8mm, the fault probability becomes zero.

Abstract

The mechanical interface has the characteristics of low shock and vibration, and is emphasized in the aerospace and ocean engineering fields. In this paper, a mechanical interface based on coupled cylindrical cam mechanisms is designed. It can achieve the expected functions, but there exist faults in some times. The fault modes and causes of the interface are firstly analyzed. Then a design approach based on Monte Carlo simulation is presented for analyzing and optimizing its reliability. According to the fault modes, the performance functions of the interface are established for obtaining the optimal scheme. A case is given to illustrate the proposed method. The simulation results and the prototype experiments prove that the optimization scheme effectively improves the reliability of the interface, and has better performance than the original one.

Keywords

mechanical interface, fault mode analysis, Monte Carlo simulation, reliability design, cylindrical cam mechanism.

Acronyms and Abbreviations

MAX	The maximum value.
MIN	The minimum value.
AVG	The average value.
RMS	Root-mean-square.
P-P	Peak-to-peak.
MCS	Monte Carlo simulation.

Notations

L_i	Horizontal length of the central block curve groove.
θ_t	The x axis coordinate of the pin shaft.
h_t	The y axis coordinate of the pin shaft.
S	Vibration displacement of the pin shaft in horizontal direction.
W	Vibration displacement of the pin shaft in vertical direction.
w	Rotational speed of the drive ring.
t	Operating time of the interface.
r_i	Outer radius of the center block.
r_o	Outer radius of the drive ring.
Lo	Length of drive ring in the rotation stage.
L_s	The distance from the farthest point of the pin shaft to the straight section of the drive ring rotation stage.
h_c	Protrusion height.
q	The protrusion length to be extended.

1. Introduction

Modular design plays vital roles in the design of large-scale complex equipment with multi-task objectives. By using the modular design, a complex equipment is divided into several units or modules, which is given different tasks. Mechanical or electrical interfaces are used to connect these units and achieve complex tasks. Modular design not only simplifies the design process, but also reduces the complexity of maintenance. Interface design is the technical premise to realize modular design. In recent years, the on-orbit assembly technology in the field of space and aviation started to use mechanical interfaces connecting different sub-satellites. The design idea presented in the project of Intelligent Building Blocks for On-Orbit Satellite Servicing and Assembly (iBOSS) in Germany is simple and easy to be used [1]. Its principle is to use a specially designed cylindrical cam structure to

(*) Corresponding author.
E-mail addresses: J-H. Li - senngiri@163.com, Z-J. Liu - liuzj@dlmu.edu.cn, D-P. Wang - 13810898248@163.com, Y. Tian - tianyun20092010@163.com, Y-C. Zhao - 1254686141@qq.com

drive the locking hook to realize mechanical, electrical and data connections. The interface design based on cylindrical cam mechanisms is the core of iBOSS.

The cylindrical cam mechanism is widely used in the engineering field [2, 8, 9, 17, 25]. In this paper, based on the iBOSS design idea, a mechanical interface based on coupled cylindrical cam mechanisms is proposed, and the prototype is manufactured. The experiments show there exists functional faults due to some influence factors, for example vibrations and manufacturing errors. The reliability can be greatly reduced if possible fault cannot be accommodated, even lead to system shut-down [17]. Thus the fault causes need to be studied.

Many researchers proposed different methods for the reliability anlaysis, for example Bayesian network, evidential network and Monte Carlo Simulation (MCS) [10, 13,14]. Rhee et al. [15] discused a new methodology of Life Cost-based FMEA. Wang et al. [21] proposed a new adaptive sampling approach for system reliability assessment with multiple dependent failure events. Xu et al. [22] put forward a new class of computational methods, referred to as decomposition methods, which has been developed for predicting failure probability of structural and mechanical systems subject to random loads, material properties, and geometry. Haldar et al. [5] raised a novel reliability evaluation method for large nonlinear engineering systems excited by dynamic loading applied in time domain. Hu et al. [7] pointed out that the first order reliability method (FORM) is difficult to solve the highly nonlinear problem, so a mixed efficient global optimization (m-EGO) method is proposed. Padmanabhan et al. [3] studied a Reliability-Based Optimization (RBO) methodology that uses MCS techniques, which provides more accurate results for highly nonlinear problems. Wang et al. [20] presented a new enhanced MCS (EMCS) approach for reliability analysis and design considering disjointed failure regions. Mayda et al. [12] proposed a systematic design framework supported by reliability analysis that it can provide an effective connection among the early design steps especially both at system level and component level by utilizing MCS. Singh et al. [16] pointed out that the traditional MCS is accurate, but computationally expensive. Therefore, they proposed a computationally efficient importance sampling technique to improve the calculation efficiency. To address the fuzzy random uncertainty in structural reliability analysis, You et al. [23] proposed a novel method for obtaining the membership function of fuzzy reliability on the two orders four central moments (TOFM) method based on envelope distribution. Hölle M et al. [6] proposed a statistical method for the evaluation of the uncertainties for pneumatic multihole probe measurements. Zhang et al. [24] proposed a finite element-based Brownian dynamics simulation (BDS) method to solve for the motion of nanofibers suspended within a viscous fluid. MCS is used to evaluate a large quantity of motions of a single fiber associated with different random Brownian forces and torques. Goka E et al. [4] analyzed the overall statistical tolerance of the over-constrained mechanical assembly by determining the assembly and the functionality probabilities based on optimization techniques combined with MCS. Liu et al. [11] proposed a reliability assessement approach based on MCS and modular sequence-enforcing fault tree model for repairable phased-mission systems. Sun et al. [18] presented a reliability model of sequence motions. The performance function of the former motion

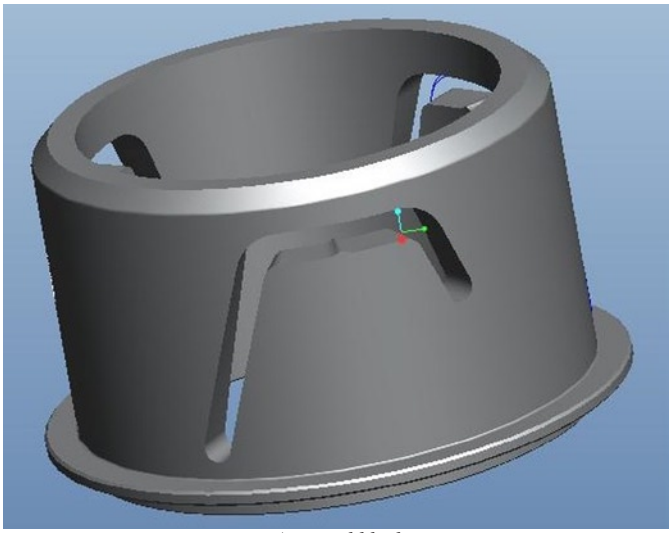

a) central block

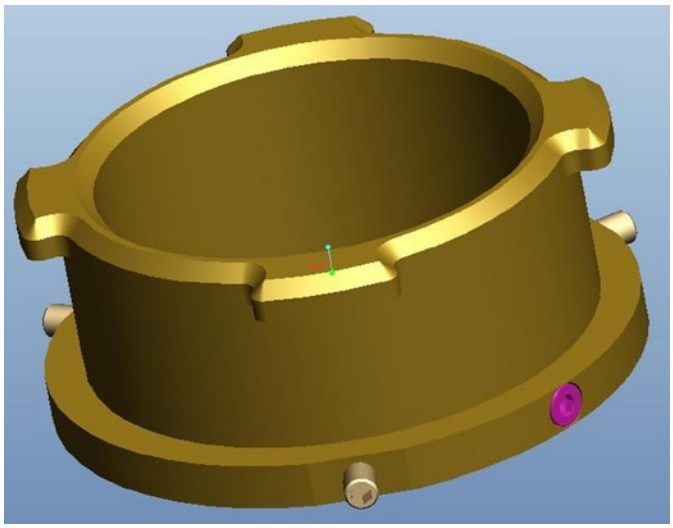

b) lock hook assembly

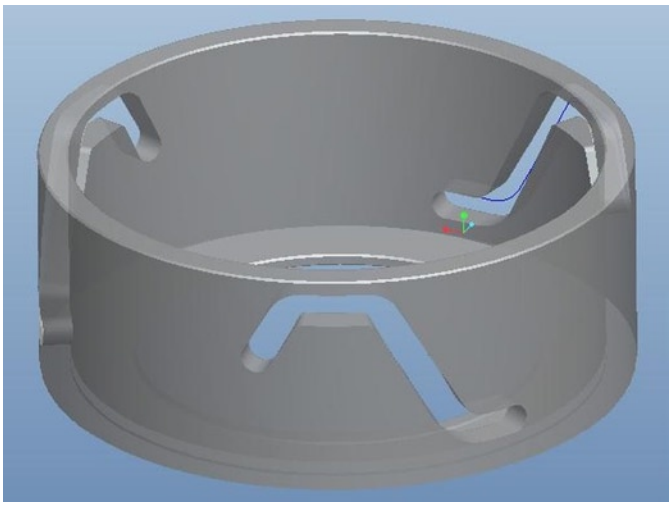

c) drive ring

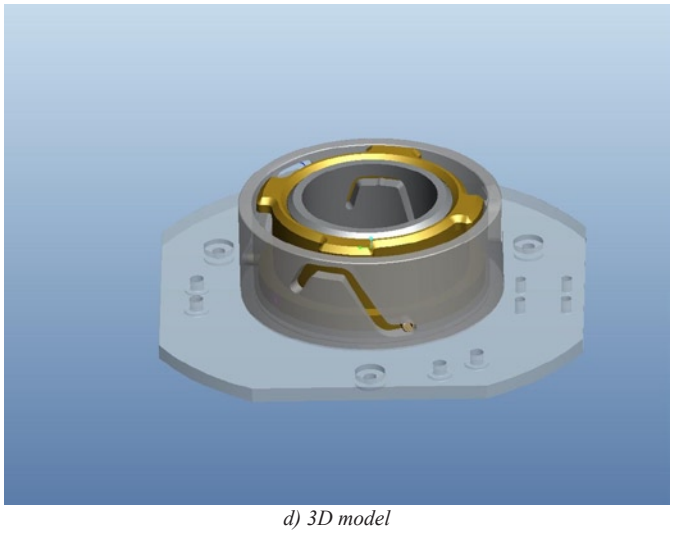

d) 3D model

Fig.1. The interface model

is regarded as just one of the influence factors of the next motion and the solving idea based on MCS is proprosed.

In summary, MCS is widely used for the reliability analysis of complex systems. In this paper, on the basis of analyzing the fault modes of the cylindrical cam mechanism motion, a reliability optimization approach based on MCS is proposed for improving the motion reliability of the interface, which is verified by simulation and prototype experiment.

2. Interface Design and Fault Mode Analysis

2.1. Interface Design and Working Principle

Based on the basic principle of cylindrical cam mechanisms and the iBOSS design idea, a mechanical interface can be designed. The core parts of this interface include central block, lock hook assembly and drive ring as shown in Fig. 1. There are curve grooves in the central block and drive ring as in Fig. 2, which can be considered as cylindrical cams.

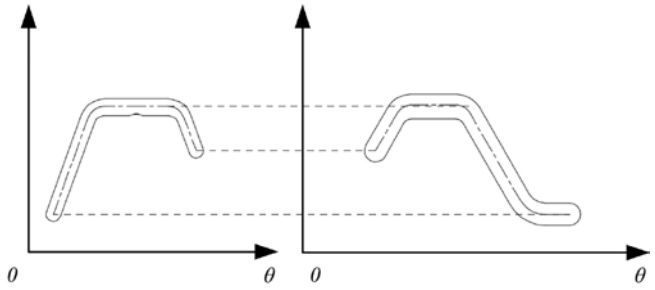

Fig.2. The curve grooves in the central block and drive ring

The central block is fixed on the bottom plate. The lock hook assembly is a driven unit, which rotates at a constant speed under a motor driving. The inner side of the pin shaft on the lock hook assembly moves on the curve groove of the central block, and the outer side moves on the curve groove of the drive ring at the same time. So the curved groove of the central block directly reflects the movement track of the lock hook assembly, and the curve grooves of the drive ring and the central block control the movement speed of the lock hook assembly. In the application, the lock hook assembly connects with another one on the other side according to a predetermined track. Each module is mounted by a interface. Thus by the drive ring motion, the interface can achieve the connection and seperation of two modules.

Under the gravity environment, the interface is placed horizontally. In order to study the movement process of the lock hook conveniently, the curve grooves of the central block and the driving ring are unfolded on the same plane, the curve grooves of the central block remains stationary, and the curve groove of the drive ring moves to the right as shown in Fig. 3. The crossing part of the two is the position of the pin shaft in the lock hook assembly. The pin shaft on one side of the drive ring is indicated by solid lines, and the pin shaft on the side of the central block is indicated by dashed lines.

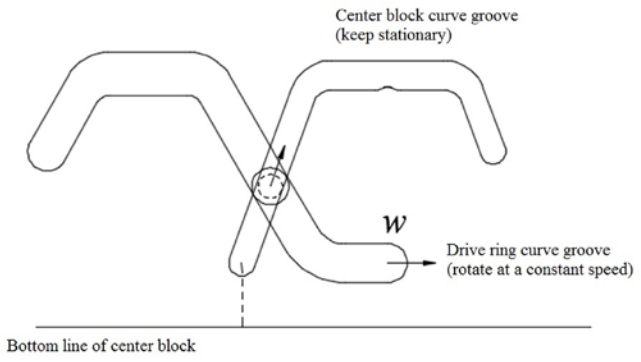

Fig. 3. Lock hook rising stage

Assuming that there are no other external influencing factors, the normal connecting process of the interface is as follows.

1) Lock hook rising stage

As shown in Fig. 3, under the driving force of the drive ring, the pin shaft on the lock hook assembly rises at a constant speed along the rising section of the curve grooves of the central block and the drive ring.

2) Lock hook rotating stage

After the lock hook rising stage is completed, the inner side of the pin shaft reaches to the straight section of the central block curve groove first. Due to the height difference between the straight sections of the two curve grooves, the outer side of the pin shaft will be stuck by the corner of the drive ring curve groove and remain relatively stationary with the drive ring, as shown in Fig. 4a).

The drive ring continues to rotate, and pushs the lock hook to rotate at a constant speed until the inner side of the pin shaft is blocked by the protrusion on the curve groove of the central block, as shown in Fig. 4b). When the drive ring continues to rotate, the lock hook will have an upward trend until the outside of the pin shaft rises to the straight section of the curve groove of the drive ring, as shown in Fig. 4c). Then the pin shaft will be stuck by the central block protrusion to stop moving relative to the drive ring, the pin shaft moves leftward along the drive ring curve groove until the outer side of the pin shaft contacts the upper wall corner of the drive ring curve groove, as shown in Fig. 4d). Then under the driving force of the drive ring, the inner side of the pin shaft passes over the protrusion, as shown in Fig. 4e). Finally, under the push of the drive ring, the lock hook and the drive ring move at the same speed together.

3) Lock hook lowering stage

The drive ring continues to push the lock hook to move at a constant speed. When the inner side of the pin shaft reaches the curve groove lowering section of the central block and the outer side of the pin shaft reaches the curve groove lowering section of the drive ring, the lock hook starts to move along the curve groove of the central block, as shown in Fig. 5. Finally, the inner side and the outer side of the pin shaft respectively reach the end points of the two sections of curve grooves, and two modules are connected and locked.

The seperating movement process is reverse. In this paper, the connectiong process is analyzed, and the analysis is similar for the seperating process.

2.2. Fault Mode Analysis of the Interface

In the actual working process, due to the existence of some influence factors, for example vibration or tolerance, the lock hook will deviate from the expected motion trajectory. As shown in Fig. 6, the intersection of the pin shaft movable range in the central block and drive ring curve grooves is considered as the movement area of the lock hook assembly. The movement areas of the pin shaft in the rising, rotating, lowering stages are obtained respectively, as shown in Figs.6-8. It can be seen that the movable areas of the pin shaft are very small in the rising and lowering stages. Even if there is large vibration, the movement process is certain, but the tolerance design should be emphasized. In the rotating phase, the possible movable area of the pin shaft is large, which may lead to uncertain movement and even motion fault of the pin shaft.

Through the force analysis and movement area of the pin shaft, it can be found that in the process of rotating stage as shown in Fig. 4c-4d, the locking hook is only limited by friction force and protrusion supporting force in the horizontal direction, and vibration is easy to make it displace. The interface falult mode can be divided into the following two situations:

1) Fault mode 1

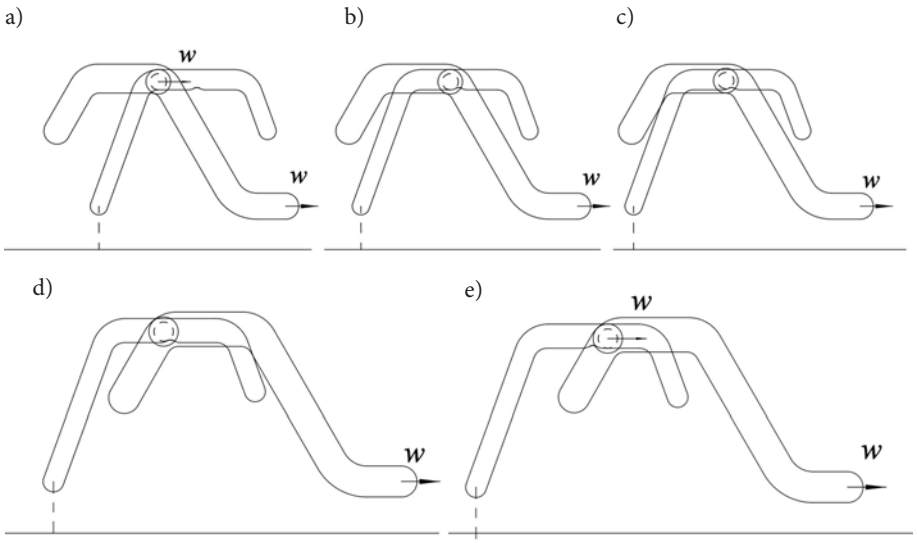

Fig. 4. Lock hook rotation stage

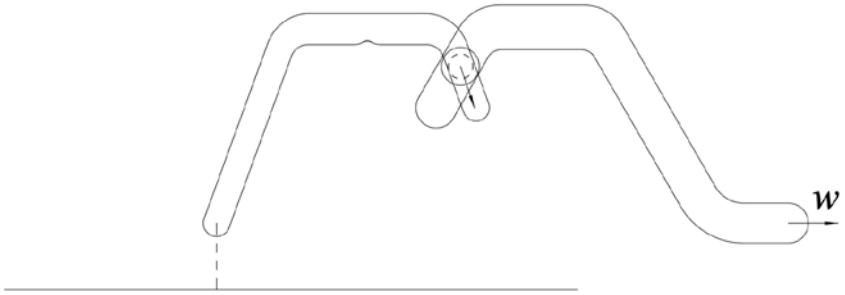

Fig. 5. Lock hook lowering stage

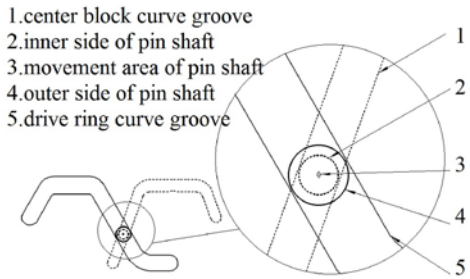

Fig. 6. Movable area of pin shaft in the rising stage

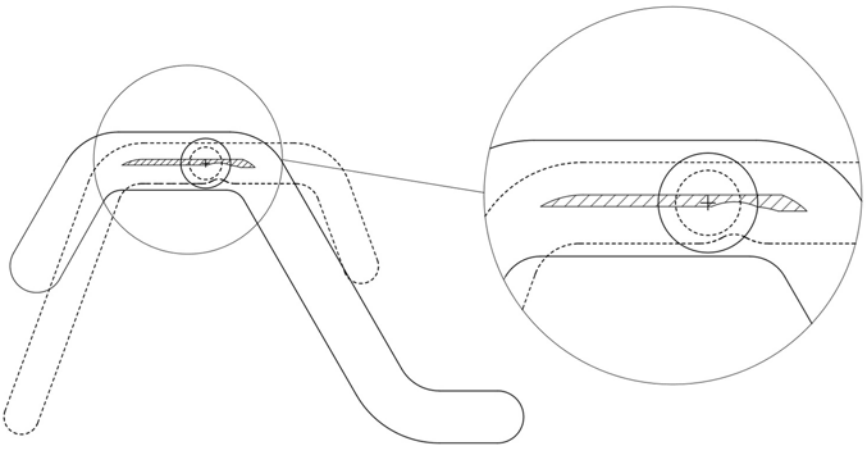

Fig. 7. Movable area of pin shaft in the rotating stage

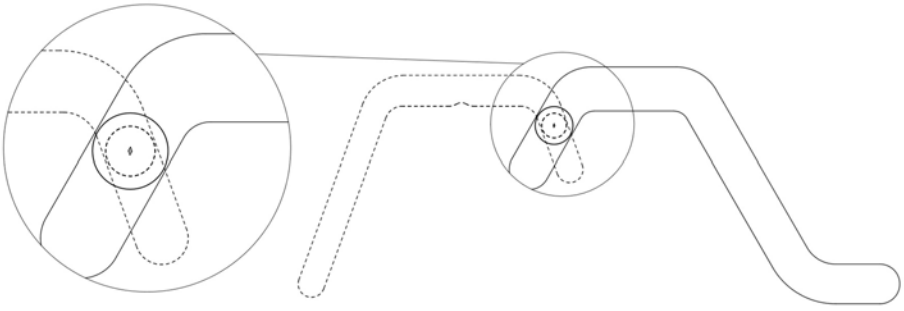

Fig. 8. Movable area of pin shaft in the lowering stage

The influence factors cause the lock hook assembly to rotate clockwise, i.e. the pin shaft moving to the left. As shown in Fig. 9, the inner side of the pin shaft will reach the rising stage of the central block curve groove, and the outer side of the pin shaft will reach the lowering stage of the drive ring curve groove. This will lead that the pin shaft descends along the curve grooves, the interface locks and cannot operate.

2) Fault mode 2

The influence factors cause the lock hook assembly rotates counterclockwise, i.e. pin shaft moving to the right. As shown in Fig. 10, the inner side of the pin shaft passes over the protrusion, the outer side of the pin shaft will reach the rising stage of the drive ring curve groove, and the inner side of the pin shaft will reach the lowering stage of the central block curve groove. This will lead that the pin shaft descends along the curve groove, the interface locks and cannot operate.

In summary, influence factors might lead to the uncertain motions of the pin shaft in the rotating stage and in turn motion faults of the interface. In this paper, the design and analysis is carried to optimize the interface reliability under uncertain influence factors.

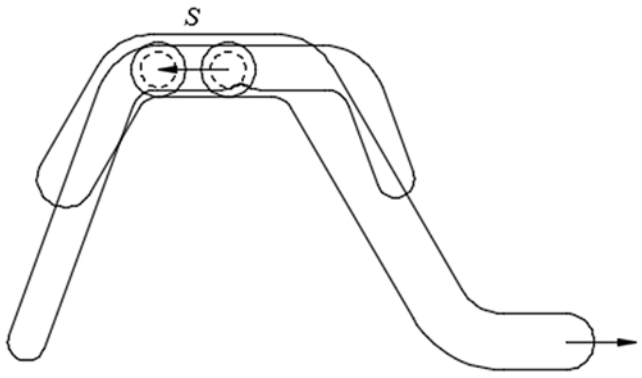

Fig. 9. Fault mode 1

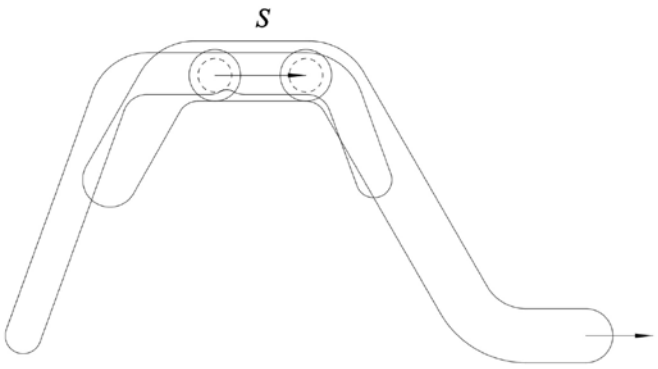

Fig. 10. Failure mode 2

3. Interface Optimization Design Based on MCS

3.1. Optimization Design Approach Based on MCS

Different from physical experiments, MCS performs random sampling and carries out a large number of experiments on computers, then observes the statistical characteristics of the experiment outputs and draw a conclusion about the model output on the basis of the statistical experiment. In each experiment, the possible values of the input random variables $X=(X_1,X_2,\cdots,X_n)$ are generated according to their distribution. Then, the value of the output variable Y is calculated by the function $Y=g(X)$ at the input random variable sample. Through many experiments in this way, a set of samples of the output variable Y can be used for statistical analysis to estimate the characteristics of the output variable Y.

According to the basic principle of MCS, the optimization process based on MCS for the interface design includes structure design, fault mode analysis, performance function establishemnt for the fault modes, input random variable distribution, MCS, output results and analysis. If the improved scheme meets the requirements, the optimal scheme is given. Otherwise, the MCS is repeated.

3.2. Performance Functions Establishment

Since the central block remains stationary and the locking hook assembly moves along the curve groove of the central block, a coordinate system is established with the central block as a reference, as shown in Fig. 11.

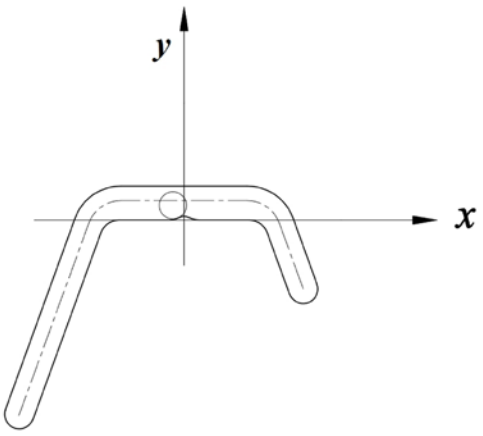

Fig. 11. The coordinate system based on the central block curve groove

Take the position of the pin shaft in Fig. 4c as the starting point, settin t=0, and the position of the pin shaft in Fig. 4d as the end point, setting $t=t_1$. The drive ring rotates with angular velocity w, thus the position of the pin shaft can be determined at any time.

Assuming that the vertical vibration displacement of the pin shaft is W and the horizontal vibration displacement is S, the relative drive ring movement displacement $S'=Sr_i/r_o$, where r_i and r_o are the maximum radii of the central block and the drive ring, respectively. When the lock hook is stuck at the protrusion part of the central block, the coordinates of the lowest point of the pin shaft are (θ_t, h_t), and θ_t is negative. The parameters are shown in Fig. 12.

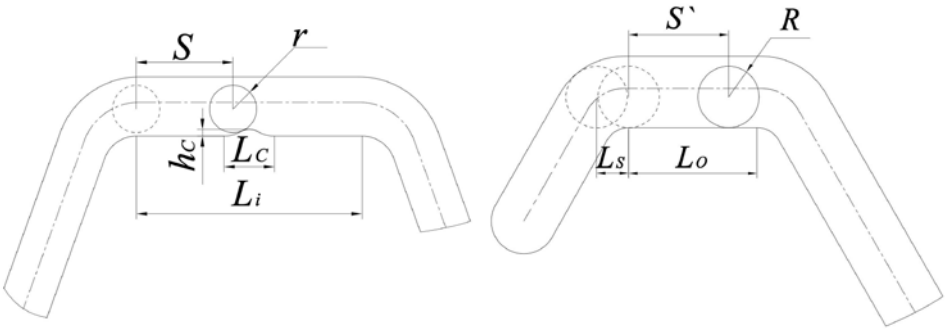

Fig. 12. Correspondence diagram of design parameters

According to the above analysis, the fault mode 1 takes place when the following conditions are met:

1) The influence factors cause the inner side of the pin shaft to rotate clockwise and reach the corner of the central block curve groove in the rising stage;
2) The outer of the pin shaft reaches the corner of the drive ring curve groove in lowering stage;
3) The outer side cannot exceed the range of the left side of the curve groove.

Thus the performance function of fault mode 1 is established, i.e. the interface fails when Eq. (1) is satisfied.

$$\begin{cases} -S > 0.5L_i + \theta_t \\ wt - Sr_i / r_o > L_o \\ L_o + L_s > wt - Sr_i / r_o \end{cases} \tag{1}$$

The fault mode 2 takes place when the following conditions are met:

1) The inner side of the pin shaft moves rightward, and passes over the protrusion;
2) The vertical amplitude is greater than the blocking height;
3) The outer side of the pin shaft reaches the corner of the drive ring curve groove in rising stage;
4) The outer side of the pin shaft cannot exceed the range of the curve groove in right side.

The interface fails when Eq. (2) is satisfied.

$$\begin{cases} S > -\theta_t \\ W > h_c - h_t \\ Sr_i / r_o - wt > 0 \\ L_s > Sr_i / r_o - wt \end{cases} \tag{2}$$

The driving ring rotates at a constant speed. In order to study the failure of the pin shaft in the whole movement process in the straight section, set the value of time t as Uniform distribution in the whole time period. The external factor affecting the movement of the interface is the motor vibration. It is assumed here that the horizontal displacement generated by the motor is normally distributed and the vertical amplitude is uniformly distributed. So the random variable distribution of the device is $t \sim U(0,t_1)$, $W \sim U(0,H\text{-}r\text{-}h_c)$, $S \sim N(E(\Delta),\sigma(\Delta))$ where t_1 is the total movement time in rotating stage, H is the width of the central block curve groove in rotation stage, $E(\Delta)$ is the mathematical expectation of the horizontal amplitude, and the horizontal amplitude variance is $\sigma(\Delta)$.

4. Case Analysis

The design parameters of the interface are as shown in Table 1.

Inputting the number of MCS, the failure probability distribution with the simulation times is obtained as shown in Table 2 and Fig. 13.

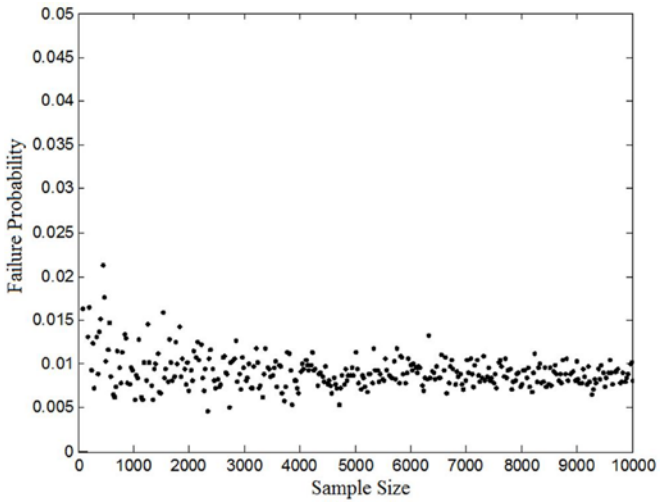

Fig. 13. Failure probability distribution with sample size

Table 2. Failure Probability Distribution with Simulation Times

Simulation Times	100	1000	10000
Number of failures(mode 1)	0	0	0
Number of failures(mode 2)	2	8	73
Failure probability	0.0200	0.0080	0.0073

From Table 2, when the horizontal amplitude is 3 mm, the estimated value of the failure probability of the interface is 0.0073, and only the fault mode 2 occurs. In order to further improve the reliability of the interface, the influence of external factors (horizontal amplitude, rotation speed of the drive ring) and self-factors (protrusion length) on the failure probability are respectively studied, as shown in Figs.14-16.

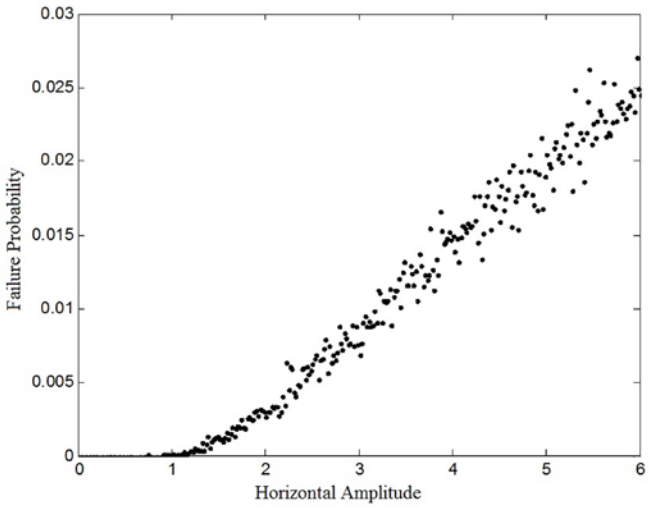

Fig. 14. Failure probability with horizontal amplitudes

From Fig. 14, the fault probability increases linearly with the horizontal amplitude. The larger the horizontal amplitude is, the higher the failure probability is. As seen from Fig. 15, the failure probability is inversely proportional to the rotation speed of the drive ring. The faster the rotation speed of the drive ring is, the lower the failure probability is. According to Fig. 16, when protrusion length is extended to 3-3.8mm, the failure probability is 0.

Therefore, the reliability of the interface can be improved by reducing the external vibration or increasing the rotating speed of the drive ring under the condition of ensuring the functional requirements. It can also be improved by increasing the protrusion length.

Table 1. The design parameter values of the case

Design parameters	values
the rotation stage movement time t_1 /s	1
central block radius r_i /mm	25
drive ring radius r_o /mm	41
length of central block curve groove in the rotation stage L_i /mm	13.4
length of drive ring curve groove in rotation stage L_o /mm	9
drive ring rotation speed w /mm/s	10.6
distance from the farthest point of the pin shaft to the straight section of the drive ring at this stage L_s /mm	2.25
the groove width of the central block rotation stage H /mm	3.5
the total length of the protrusion L_c /mm	3
the height of the protrusion h_c /mm	0.4
the coordinates of the lowest point of the pin shaft /mm	(-0.96, 0.2)
the range of horizontal amplitude S /mm	(-3,3)

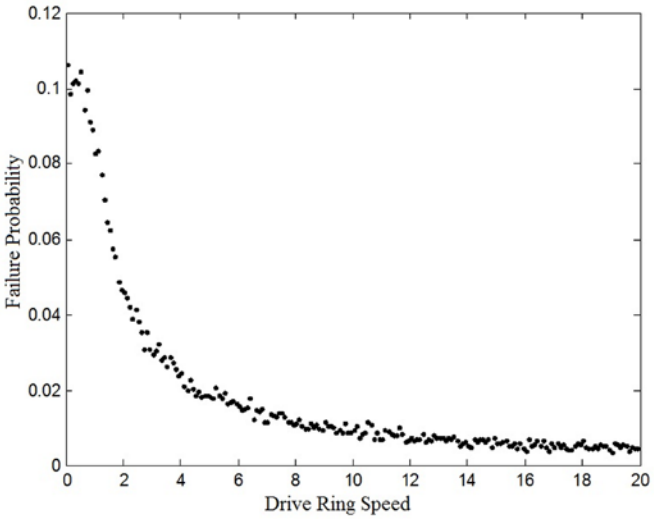

Fig. 15. Failure probability with drive ring speeds

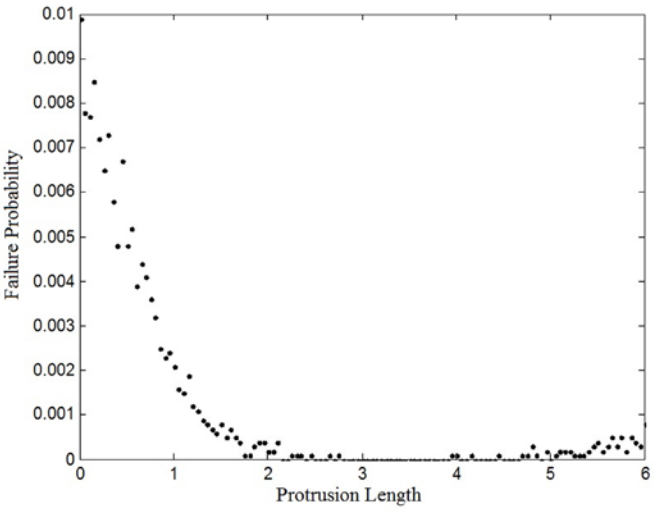

Fig. 16. Failure probability with protrusion lengths

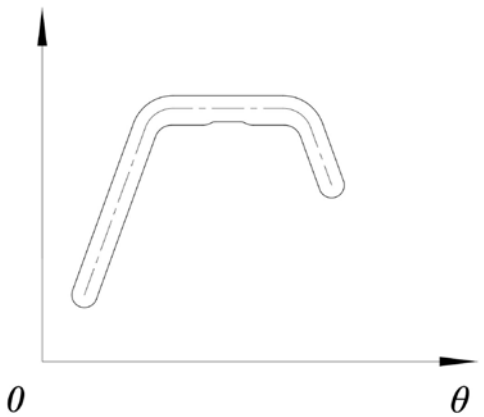

Fig. 17. Curve groove of new central block

According to the above analysis, on the premise of not changing other parameters, the protrusion of the central block curve groove is extended to 3 mm, which is shown in Fig. 17.

The corresponding performance functions of the new curve groove are obtained.

The fault mode 1:

$$\begin{cases} -S > 0.5L_i + \theta_t + 0.5q \\ wt - Sr_i / r_o > L_o \\ L_o + L_s > wt - Sr_i / r_o \end{cases} \tag{3}$$

The fault mode 2:

$$\begin{cases} S > -\theta_t + q \\ W > h_c - h_t \\ Sr_i / r_o - wt > 0 \\ L_s > Sr_i / r_o - wt \end{cases} \tag{4}$$

When q=3, the functions cannot be satisfied regardless of any values of amplitude S (-3,3), which indicates that faults will not occur. The results are verified by MCS.

An experiment was carried to verify the simulink results. The running process of connecting and seperating is considered as a test. If there is any motion fault, record a failure, and repeats the tests for 1000 times to obtain the comparison of failure times between the optimized scheme and the original scheme. The test results are listed in Table 3.

Table 3. Failure Test Results

Test Times	10	100	500	1000
Original scheme failure /times	0	2	6	11
	1	3	6	9
Optimization scheme failure /times	0	0	0	0
	0	0	0	0

5. Prototype Test

The acceleration sensors are used to test the vibration of the interface prototype in the vertical direction during operation. The test is divided into two groups, i.e., group A is for the original scheme under normal gravity, and group B is for the optimization scheme. Each group tests 18 times. The test results in the connecting process are shown in Fig. 18-20.

The following conclusions can be drawn from Figs.18-20.

1) The maximum value of group B is smaller than that of group A, while the minimum value is larger than that of group A. This conclusion can also be drawn from the peak-to-peak comparison.
2) The average value of group B is smaller than that of group A on the whole, indicating that the vibration generated in the whole process of group B is smaller.
3) The root mean square of group B is smaller than that of group A, which indicates that the dispersion degree of group B is smaller than that of group A, i.e. the vibration generated at the protrusion is less obvious than that of the whole process.

Similar conclusions can be obtained for the seperating process.

6. Conclusions

In this paper, a motion fault analysis method based on MCS is proposed for the interface based on cylindrical cam mechanisms. By analyzing the working principle of the interface, the fault modes and performance functions are established. The functions are calculated by MCS to determine the failure rule and obtain the optimization scheme.

The analysis results of the case show the failure probability increases linearly with the horizontal amplitude. The failure probability is inversely proportional to the rotation speed of the drive ring. When the protrusion length is extended to 3-3.8mm, the failure probability of the interface is zero.

According to the analysis results, an optimization scheme is given. MCS and experimental test results show that the optimization scheme is feasible. The comparisons of two group test results confirm that

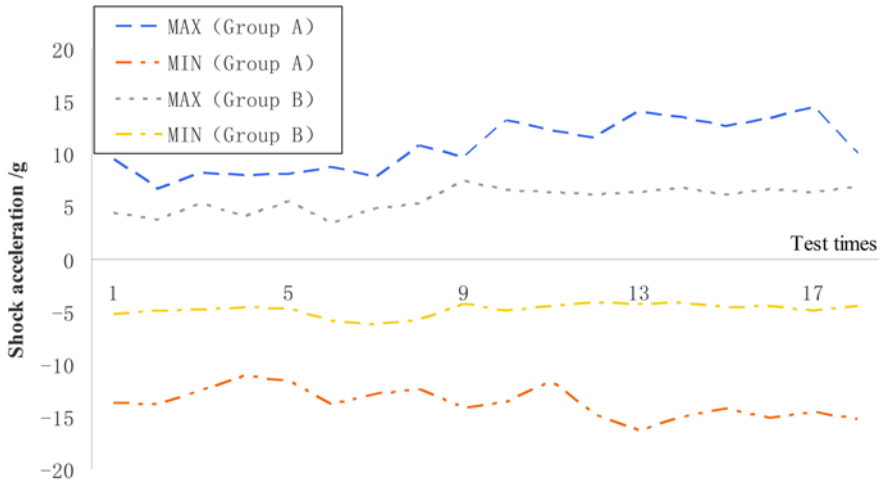

Fig. 18. MAX&MIN in the connecting process

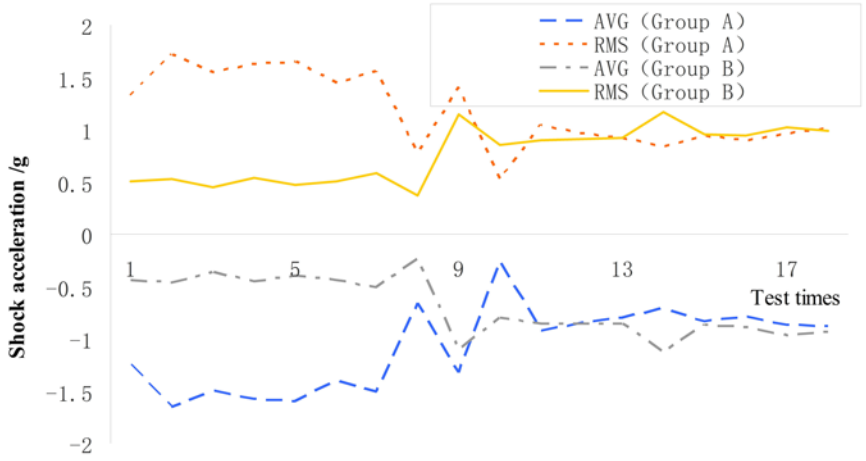

Fig. 19. AVG&RMS in the connecting process

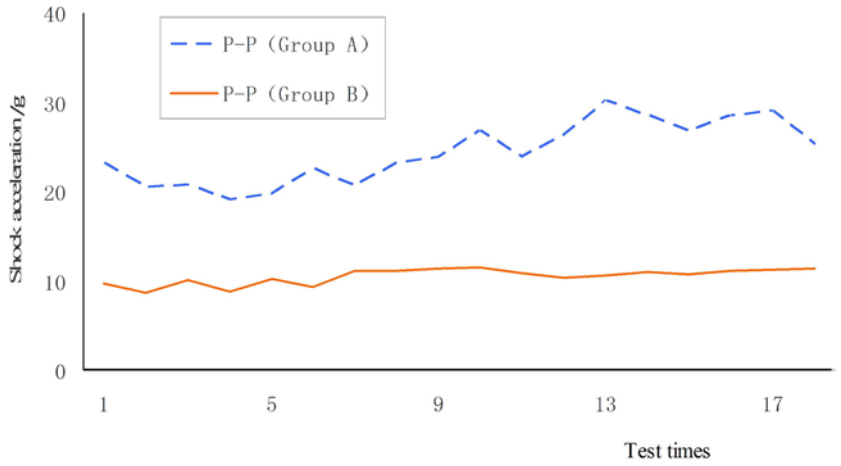

Fig. 20. P-P in the connecting process

the optimization scheme has better performance than the original scheme.

This paper mainly analyzes the vibration influence, and the influence rules of other factors, for example the friction and torelance, can be further studied in the future.

Acknowledgement

This work was supported by National Natural Science Foundation of China under grant 51879026; Dalian Science and Technology Innovation Fund Project under grant 2020JJ25CY016; Fundamental Research Funds for the Central Universities of China under grant 3132019308.

References

1. Adomeit A, Lakshmanan M, Schervan T, Dafnis A, Reimerdes H G. Structural concept and design for modular and serviceable spacecraft systems. Collection of Technical Papers - AIAA/ASME/ ASCE/AHS/ASC Structures, Structural Dynamics and Materials Conference; 2013, https://doi.org/10.2514/6.2013-1575.
2. Carvalho T H M, Kingston J. Establishing a framework to explore the Servicer-Client relationship in On-Orbit Servicing. Acta Astronautica 2018; 153: 109-121, https://doi.org/10.1016/j.actaastro.2018.10.040.
3. Feng X, Moon I, Ryu K. Revenue-sharing contracts in an N-stage supply chain with reliability considerations. International Journal of Production Economics 2013; 147: 20-29, https://doi.org/10.1016/j.ijpe.2013.01.002.
4. Goka E, Homri L, Beaurepaire P, Dantan J Y. Statistical tolerance analysis of over-constrained mechanical assemblies with form defects considering contact types. Journal of Computing and Information Science in Engineering 2019; 19(2): 021010, https://doi.org/10.1115/1.4042018.
5. Haldar A, Farag R. A novel reliability evaluation method for large dynamic engineering systems. 2010 2nd International Conference on Reliability, Safety and Hazard; 2010: 21-31, https://doi.org/10.1109/ICRESH.2010.5779619.
6. Hölle M, Bartsch C, Jeschke P. Evaluation of measurement uncertainties for pneumatic multihole probes using a Monte Carlo method. Journal of Engineering for Gas Turbines and Power 2017; 139(7): 072605, https://doi.org/10.1115/1.4035626.
7. Hu Z, Du X. Mixed efficient global optimization for time-dependent reliability analysis. Journal of Mechanical Design 2015; 137(5): 051401, https://doi.org/10.1115/1.4029520.
8. Kortmann M, Meinert T, Dafnis A, Schroeder K. Multifunctional interface for modular satellite systems with robotic servicing capabilities. Proceedings of the International Astronautical Congress 2018; 15: 9726-9734, https://doi.org/10.1007/s42423-018-0009-1.
9. Li W J, Cheng D Y, Liu X G, Wang Y B. On-orbit service (OOS) of spacecraft: A review of engineering developments. Progress in Aerospace Sciences 2019; 108: 32-120, https://doi.org/10.1016/j.paerosci.2019.01.004.
10. Li Y F, Huang H Z, Mi J, Peng W, Han X. Reliability analysis of multi-state systems with common cause failures based on Bayesian network and fuzzy probability. Annals of Operations Research 2019; https://doi.org/10.1007/s10479-019-03247-6.
11. Liu C X, Kramer A, Neumann S. Reliability assessment of repairable phased-mission system by Monte Carlo Simulation based on modular sequence-enforcing fault tree model. Eksploatacja i Niezawodnosc - Maintenance and Reliability 2020; 22(2):272-281, https://doi.org/10.17531/ein.2020.2.10.
12. Mayda M, Choi S K. A reliability-based design framework for early stages of design process. Journal of the Brazilian Society of Mechanical Sciences and Engineering 2017; 39(6): 2105-2120, https://doi.org/10.1007/s40430-017-0731-y.
13. Mi J, Beer M, Li Y F, Broggi M, Cheng Y. Reliability and importance analysis of uncertain system with common cause failures based on survival signature. Reliability Engineering & System Safety 2020; https://doi.org/10.1016/j.ress.2020.106988.
14. Mi J, Li Y F, Peng W, Huang H Z. Reliability analysis of complex multi-state system with common cause failure based on evidential networks. Reliability Engineering & System Safety 2018; 174: 71-81, https://doi.org/ 10.1016/j.ress.2018.02.021.
15. Rhee S J, Ishii K. Predicting cost of poor quality and reliability for systems using failure modes and effects analysis. American Society of Mechanical Engineers 2004; 117: 23-33, https://doi.org/10.1115/IMECE2004-59612.
16. Singh A, Mourelatos Z P, Nikolaidis E. An importance sampling approach for time-dependent reliability. Proceedings of the ASME Design Engineering Technical Conference 2011; 5: 1077-1088, https://doi.org/10.1115/DETC2011-47200.
17. Stetter R, Goser R, Gresser S, Till M, Witczak M. Fault-tolerant design for increasing the reliability of an autonoumous driving gear shifting system. Eksploatacja i Niezawodnosc - Maintenance and Reliability 2020; 22(3):482-492, https://doi.org/10.17531/ein.2020.3.11.
18. Sun Y, Sun Z L, Yin M G, Zhou J. Reliability model of sequence motions and its solving idea. Eksploatacja i Niezawodnosc - Maintenance and Reliability 2019; 21(3):359-366, https://doi.org/10.17531/ein.2019.3.1.
19. Tanaka H, Yamamoto N, Yairi T, Machida K. Autonomous assembly of cellular satellite by robot for sustainable space system. International Astronautical Federation - 56th International Astronautical Congress 2005; 7: 4844-4854, https://doi.org/10.20965/jrm.2006.p0356.
20. Wang P, Cui X, Wang Z. Reliability analysis and design considering disjointed active failure regions. ASME 2015 International Mechanical Engineering Congress and Exposition 2015; 11, https://doi.org/10.1115/IMECE2015-52985.
21. Wang Z, Wang P. An integrated performance measure approach for system reliability analysis. Journal of Mechanical Design, Transactions of the ASME 2015; 137(2): 021406, https://doi.org/10.1115/1.4029222.
22. Xu H, Rahman S. Decomposition methods for structural reliability analysis. Probabilistic Engineering Mechanics 2005; 20(3): 239-250, https://doi.org/10.1016/j.probengmech.2005.05.005.
23. You L, Zhang J, Li Q, Ye N. Structural reliability analysis based on fuzzy random uncertainty. Eksploatacja i Niezawodnosc - Maintenance and Reliability 2019; 21 (4): 599-609, http://dx.doi.org/10.17531/ein.2019.4.9.
24. Zhang D, Smith D E. Finite element-based brownian dynamics simulation of nanofiber suspensions using Monte Carlo Method. Journal of Micro and Nano-Manufacturing 2015; 3(4): 041007, https://doi.org/10.1115/1.4031492.
25. Zimmermann J, Sadeghi M Z, Schroeder K U. The effect of γ-radiation on the mechanical properties of structural adhesive. International Journal of Adhesion and Adhesives 2019; 93:102334, https://doi.org/10.1016/j.ijadhadh.2019.01.028.